Lasers in Surgery and Medicine 20:119–130 (1997)

Laser Photoablation of Experimental Post-Infarction Ventricular Tachycardia Guided by Three Dimensional Activation Mapping

Guanglie Wu,* MD, Robert H. Svenson, MD, Laszlo Littmann, MD, Chi Hui Chuang, MD, Michelle Thompson, BS, Glenn A. Nanney, MS, Robert Splinter, PhD, George P. Tatsis, MS, and Kathy R. Dezern, RVMT

Laser and Applied Technologies Laboratory, Carolinas Heart Institute, Carolinas Medical Center, Charlotte, North Carolina 28232

Background and Objective: **The purpose of this study was to evaluate the efficacy of epicardially delivered laser energy to ablate induced ventricular tachycardia in a post-infarction canine model.**
Study Design/Materials and Methods: **In 13 canines, the left anterior wall myocardial infarction was created. Five days later, 240 plunged electrodes were inserted into the heart. Three-dimensional ventricular activation sequences were analyzed on line by a computerized mapping system.**
Results: **Sixteen sustained monomorphic ventricular tachycardias were reproducibly induced in 10 canines. Epicardially contacted Nd:YAG laser irradiated the areas of the final pathway in macro-reentrant activation and the impulse origin in focal excitation. Linear photocoagulation lesions (11–16 × 50–72 mm) were created. Seven macro-reentrant circuits and six of nine focal origins were eliminated (success rate 81%). Pathology showed that laser photocoagulation involved all surviving subepicardial and intramural fibers.**
Conclusion: **Epicardially delivered laser energy in conjunction with electrical activation mapping has a high probability of ablating post-infarction ventricular tachycardia. Lasers Surg. Med. 20:119–130, 1997.** **© 1997 Wiley-Liss, Inc.**

Key words: ablation; myocardial infarction; Nd:YAG laser; ventricular tachycardia

INTRODUCTION

Sudden cardiac death following ischemic heart disease is most frequently the result of ventricular fibrillation (VF) that is often preceded by ventricular tachycardia (VT) [1–2]. In spite of years of research, ablation of malignant VT remains a significant theoretical and clinical problem [3–11]. The success rate in map-directed catheter ablation of VT is still very low (20.6%) [3]. Possible explanations are: (1) the activation sequences of VT are incompletely identified due to limited mapping resolution; (2) arrhythmogenic substrates are incompletely ablated due to the limitation of energy sources; or (3) one or more arrhythmogenic areas are ablated, but additional sites remain.

Experimental and clinical studies have revealed that multiple activation patterns of VT are present in healed or healing myocardial infarction hearts [12–17]. The abnormal conduction pathway

Presented in part at the 15th Annual Meeting of American Society for Laser Medicine and Surgery, April 2–4, 1995, San Diego, CA.

*Correspondence to: Guanglie Wu, M.D., Laser and Applied Technologies Laboratory, P.O. Box 32861, Charlotte, NC 28232.

Accepted for publication 26 February 1996.

in variable rhythms may be more completely identified by advanced computerized three-dimensional (3-D) cardiac mapping [12–13,16–17]. This method will be helpful in guiding VT ablation.

Nd:YAG laser has been proven to be an effective energy source in the ablation of VT. Laser irradiation can successfully ablate malignant VTs in patients in the operating room [5–6,18–19]. Epicardially delivered laser irradiation can result in deep, transmural myocardial coagulation lesions [5–6,18–20].

The purpose of this study was to evaluate the efficacy of epicardially delivered laser energy to ablate induced, sustained monomorphic VT guided by 3-D cardiac mapping in a subacute myocardial infarction animal model.

MATERIALS AND METHODS

Thirteen mongrel dogs of either sex (20–30 kg) were anesthetized with 10–15 mg/kg thiopental and 1–3% isoflurane, intubated, and mechanically ventilated [Servo Ventilator 900C, Siemens, Sweden). Arterial blood pressure of a femoral artery, surface electrocardiogram (ECG) and body temperature were monitored during experiments (Monitor 90603A, Spacelab, Redmond, WA). The methods of establishing a subacute myocardial infarction canine model, 3-D cardiac mapping and programmed electrical stimulation (PES) have been presented in detail previously [12–13,21]. Briefly, the proximal left anterior descending coronary artery (LAD) was occluded by inflation a percutaneous coronary angioplasty balloon catheter for 2 hours, followed by reperfusion. Five days later, the dogs were re-anesthetized, intubated, and mechanically ventilated. A mid-sternotomy was performed and the heart was supported in a pericardial cradle. Plunge needle electrodes were constructed of 22-gauge hypodermic needles, each containing eight Teflon-insulated tungsten wires 50 μm in diameter. The left ventricular (LV) and septal needles had an interpole spacing of 1 mm, and 2–3 mm (LV needle) or 3–4 mm (septal needle) between pairs. The distance between electrodes in the right ventricular (RV) needles was 0.5 mm. In eight canines, both left and right ventricular activation mapping was performed (global mapping) [21]. Sixty plunge needles, arranged in five rows perpendicular to the long axis of the heart, were placed into the LV walls (n = 44), anterior and inferior septum (n = 8), and anterior and inferior walls of the RV along the septum (n = 8). Therefore, the ventricles were divided into five parts by five-row needles [21]. Three-dimensional ventricular activation sequences were simulated by five 2-D planes from the base to the apex, from the epicardial to endocardial layer (Fig. 2) [21]. In five dogs, relatively high density mapping of the anterior wall of the LV was performed (regional mapping) [21]. A total of 54 needles, nine needles each in six rows, were inserted into the anterior wall of the LV and the anterior septum. Another six needles were placed in the free wall of the RV along the septum. Three-dimensional activation sequences of the regional ventricular wall were simulated by four-plane maps from the subepicardial to the subendocardial layer, from the base to the apex (Fig. 5) [21]. The first row of needles was always at the base of both ventricles corresponding to normal myocardial area. The second row was located at the border zone of the infarct area, and subsequent rows were placed in the infarct area [21]. Four bipolar electrode pairs in each needle allowed recording of subendocardial (electrogram 1), intramural (two layers, electrograms 2 and 3), and subepicardial (electrogram 4) myocardial activation [21]. During the experiment, warm (37°C) saline was applied to the epicardium intermittently to prevent surface cooling and dry.

Surface ECG and 240 intramural bipolar electrograms were simultaneously amplified, filtered (band width 0.2 to 300 Hz), multiplexed at a sampling rate of 1 kHz, A/D converted, and saved by a 255-channel computerized cardiac mapping system (Cardiomapp, Arrhythmia Research Technology, Austin, TX) [12–13,21]. Computer derived activation times were assigned based on the maximum amplitude criterion in reference to the onset of the QRS complex in the surface ECG. An amplitude threshold of 0.25 mV was considered indicative of activation of tissue by the depolarizing wave front [16–17]. After on-line reviewing the electrical signals, the activation times of all sites were assigned to their respective locations in 3-D maps. Color-coded five-plane (global mapping) or four-plane (regional mapping) of ventricular isochronal activation maps were generated [21].

After a stabilization period of 30 minutes, VT was attempted to be induced by PES or burst pacing (EP-2 Clinical Stimulator, Hi-tronics Designs, Budd Lake, NJ) [12–13]. Stimulation was performed at a pulse width of 2–4 milliseconds (ms) and at twice the diastolic threshold current (0.4–1.0 mA). A hand-held epicardial bipolar probe was used for epicardial stimulation at var-

TABLE 1. Nd:YAG Laser Ablation of Induced Ventricular Tachycardias*

	VT		Photocoagulation		
Patterns	(n)	CL (ms)	Dosage (joules)	Size (mm^2)	Success rate (%)
Reentry	7	175 ± 17	6,741 ± 1,508	750 ± 165	100
Focal	9	193 ± 38	6,834 ± 4,042	691 ± 151	67
P		NS	NS	NS	

*CL, cycle length; Reentry, macro-reentrant ventricular tachycardia; Focal, focal ventricular tachycardia.

ious locations. A train of eight basic driving beats (S1) at a cycle length of 300 or 250 ms was followed by up to four decremented premature stimuli (S2-S5).

Laser source was a continuous wave Nd: YAG laser (MediLas II, Medilase, Minneapolis, MN) at the 1,064 nm wavelength. The delivery system consisted of a 400 μm bare optical fiber fed through a plastic tube. A continuous low rate saline drip at 5 ml/min was flushed through the tube. Epicardially contacted laser irradiation was performed by manually holding the optical fiber complex perpendicular to the surface of the heart [20]. Laser irradiation at the fiber tip was set at 50 or 60 watts with 10 seconds pulses.

Histopathology

At completion of the experiment, plunge needles were removed and the heart was fibrillated by a 9-volt battery. The excised heart was rinsed in normal saline, immersed and fixed in formalin solution for subsequent histopathologic examination. The epicardial sites of the needles were marked by India ink. The sizes of photocoagulation lesions on the epicardial surface were estimated. Paraffin-embedded blocks containing the lesions were sectioned perpendicular to the epicardial surface and were stained with hematoxylin-eosin and Masson's trichrome stain.

Data and Statistical Analyses

Macro-reentrant VT was identified when: 1) there was continuous electrical activity spanning the systolic and diastolic intervals; 2) the site of origination was spatially and temporally adjacent to the site of termination [12–17]. Focal VT was identified when the excitation demonstrated radial spread of activation and was spatially and temporally remote from the site of termination [16–17]. A focal pattern does not exclude the possibility of an underlying micro-reentry. Sustained monomorphic VT was assigned to that VT with monomorphic QRS complexes was reproducibly induced at least three times and lasted for more than 20 seconds. When a given morphologic VT could no longer be induced on various locations

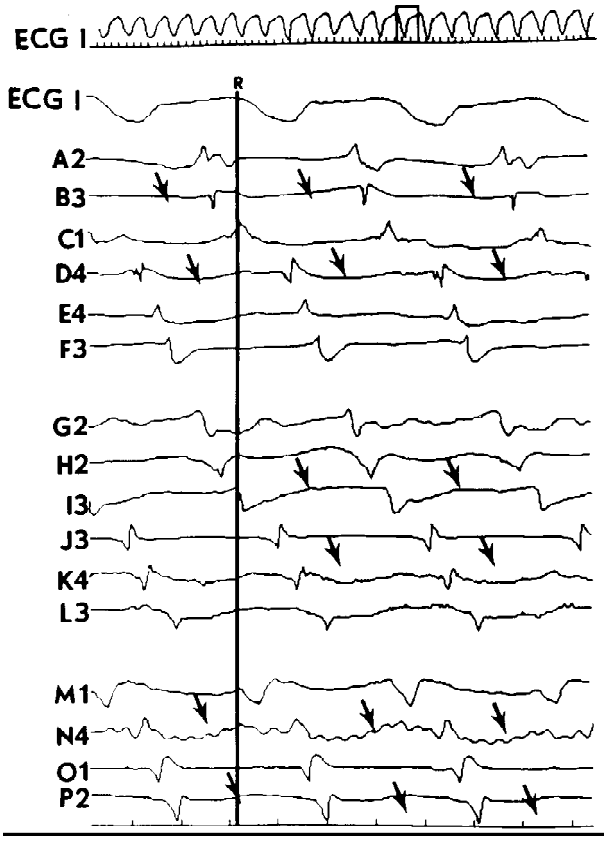

Fig. 1. Multiple selected intramural electrograms and surface ECG lead I during induced sustained monomorphic ventricular tachycardia before photoablation. Multiple intramural electrograms show the activation sequences from the earliest activation (A2 and G2) to the latest (F3, L3, and P2). The conduction directions are indicated by arrows. In this and subsequent electrogram figures, "S" indicates the stimulated beats, "R" indicates the onset of the QRS complexes in the surface ECG as the reference time of the intramural electrograms. Electrograms derived from plunged electrodes are indicated by capital letters and numbers 1–4, which are from the subendocardium to subepicardium in the ventricular wall. The electrode positions in the heart are indicated in the correspondence 3-D activation map. A unit in time scales is 50 milliseconds.

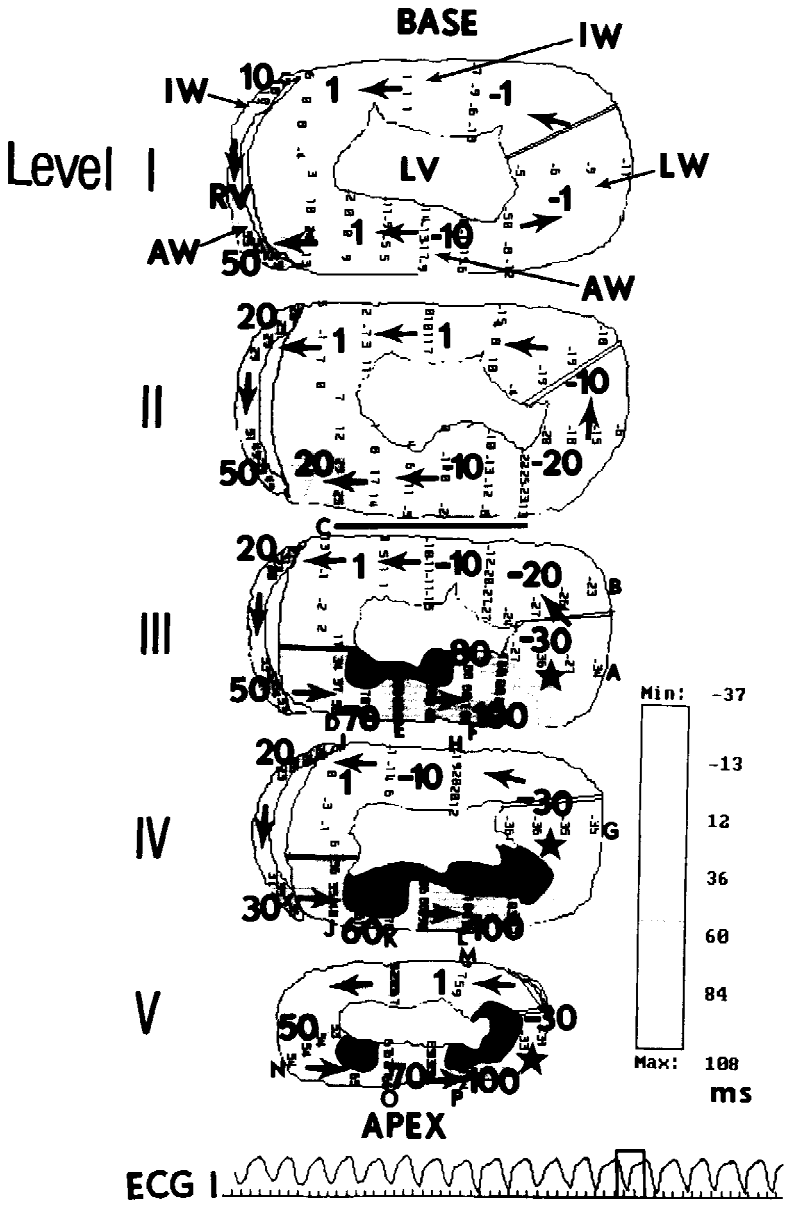

Fig. 2. Three-D ventricular activation map of a beat (outlined in ECG lead I) during the same run of VT in Figure 1 before photoablation. This figure illustrates that wave fronts originate from the areas of the earliest activation (asterisks and −30 ms), counter-clockwise propagate around the inferior and anterior walls of both ventricles to form a reentrant circuit (arrows). In this and subsequent global mapping maps, five 2-D planes were derived from five rows of needles inserted into both ventricles. The blank areas indicated by "LV" or "RV" represent the cavities of the left or right ventricle. Areas of conduction block are indicated by blackened areas or thick black lines. Arrows indicate the propagation directions of the wave fronts. Surface ECG lead I is displayed in the figure. Numbers within the map indicate local activation times of the intramural myocardium in milliseconds reference to the onset of the QRS complex in the surface ECG. Base, base of ventricles; Apex, apex of the left ventricle; AW, anterior wall; LW, lateral wall; IW, inferior wall; RV, right ventricle; LV, left ventricle; ms, milliseconds.

after photocoagulation, the VT was considered to be successfully eliminated.

Statistical data were expressed as mean ± SD. Comparisons of values for arterial blood pressure and heart rate before and after needle insertion were performed by paired Student's t-test. A difference was statistically considered significant if $P<0.05$.

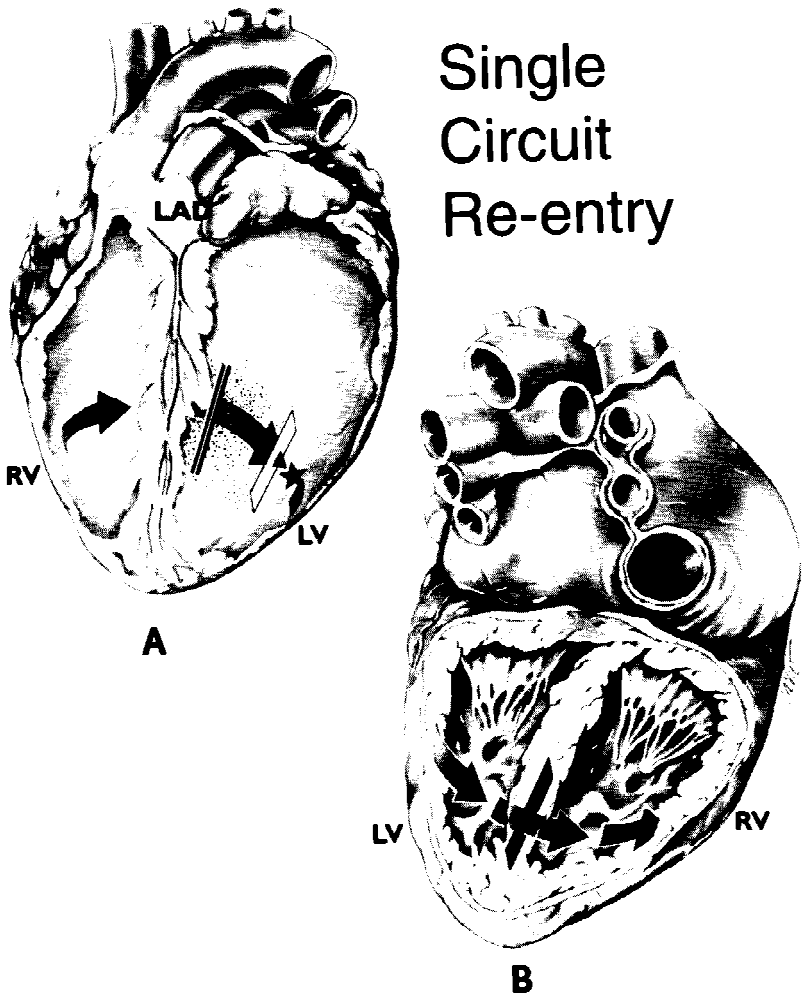

Fig. 3. Schematic illustration of the heart in the front (**A**) and back (**B**) view. This illustration indicates the activation sequences of the macro-reentrant VT in Figure 2. The lines in black and white indicate the position of photocoagulation lesion in the heart. RV, right ventricle; LV, left ventricle; LAD, left anterior descending coronary artery.

RESULTS

Insertion of 60 plunge needles into 13 myocardial infarction canine hearts did not significantly alter arterial systolic blood pressures (before insertion: 82±11 mmHg; 1 minute after insertion: 90±15 mmHg; 30 minutes after insertion: 91±14 mmHg, $P>0.05$); diastolic blood pressures (49±9 vs. 53±9 vs. 51±8 mmHg, $P>0.05$) and mean blood pressures (59±8 vs. 64±9 vs. 64±9 mmHg, $P>0.05$). Heart rates, however, increased significantly during a 30-minute stabilization period from 108±16 to 119±15 to 128±22 beats/min ($P<0.05$).

Three dogs were excluded from the results since sustained monomorphic VT was not introduced. In the remain 10 canines, 16 distinct morphologic VTs were reproducibly induced, in which seven VTs displayed the features of macro-reentrant pattern and another nine VTs demonstrated focal excitation (Table 1). Both macro-reentrant and focal VTs could be induced in five dogs. There were no significant differences in cycle length of induced VT, laser dosage and epicardial photocoagulation lesion size between reentrant and focal VTs (Table 1). All of these lesions were in linear shape. Epicardially delivered Nd:YAG laser successfully ablated 13 of 16 morphologic VTs in 10 canines (success rate 81%) (Table 1). Three canines had a second induced morphologic VT. In those cases, the hearts went into failure from the combined effects of myocardial infarction, repeated induction of VT, and laser ablation.

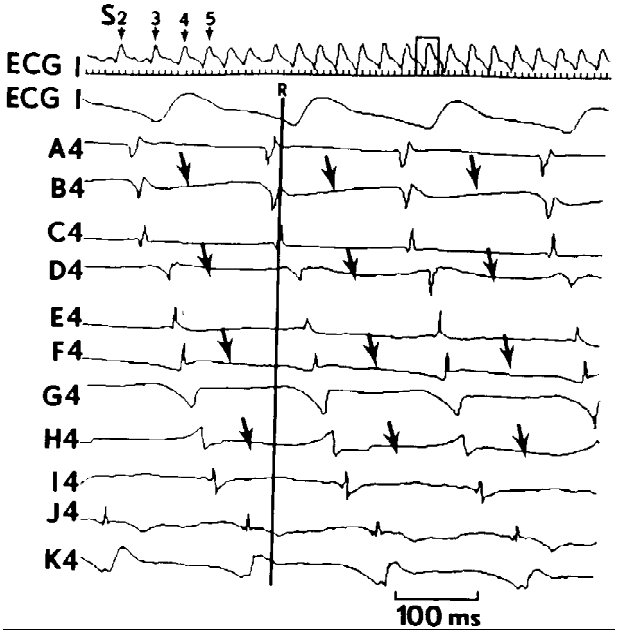

Fig. 4. Surface ECG lead I and multiple selected intramural electrograms during post-infarction VT before photoablation. Electrograms derived from the plunged electrodes in the subepicardial layer indicate the activation sequences from the earliest activation (A4) to the latest (K4).

Photoablation of Macro-Reentrant Ventricular Tachycardias

All seven of induced VTs with macro-reentrant activation patterns were successfully ablated by Nd:YAG laser energy. Each macro-reentrant pattern had its own conductive pathway and ablation features. These are two examples. Sustained monomorphic VT with a cycle length of 155 ms was reproducibly induced by PES (S1-S4: 300-160-140-170 ms) (Fig. 1, ECG lead I). Multiple selected intramural electrograms from A2 to P2 in Figure 1 demonstrate that: 1) the earliest activation originated from the mid-diastolic interval (electrograms A2, B3, G2, and H2); 2) the activation conducted from the earliest to the latest sites (electrograms F3, L3, and P2). A 3-D isochronal activation map of a beat during VT in Figure 2 illustrates activation times of the local myocardium, activation sequences in both ventricles, and ventricular locations of the selected electrograms in Figure 1 (letters A to P). The areas of the earliest activation, −30s ms before the onset of the QRS complex of the surface ECG, were located at the lateral wall of the LV (asterisks on levels III, IV, and V), which was the border zone of the infarcted anterior wall. Wave fronts propagated counterclockwise from the lateral wall to the inferior wall of the LV and septum, went through the inferior and anterior wall of the RV, crossed the anterior septum, finally depolarized the myocardium in the infarcted anterior wall of the LV (arrows on levels III, IV, and V in Fig. 2). The latest activation in the infarcted areas would reenter the sites of origin and form a reentrant circuit. The orientation of the final pathway of the circuit was from the RV to LV. Schematics of the heart illustrates the reentrant activation sequences of the VT on the front and back view of the heart (Fig. 3A,B). Nd:YAG laser irradiated the myocardium in the anterior wall of the LV along the septum to form a linear lesion (14 × 72 mm), with a total laser energy of 6,288 joules. The linear lesion was transected the final pathway of the reentrant circuit (black and white lines in Fig. 3A). The identical morphologic VT could no longer be induced after sequential induction and ablation.

A run of sustained monomorphic VT was reproducibly induced by PES (S1-S4; 250-210-160-160 ms) in a dog (Fig. 4). Multiple selected intramural electrograms in Figure 4 show that electrical activity spanned the entire systolic and diastolic intervals (electrograms A4 to K4). A regional 3-D activation map, derived from 240 plunged electrodes inserted into the infarcted anterior wall and the adjacent areas, demonstrates that the earliest activation originated from the subepicardial level of the right anterior wall along the septum (asterisk on the subepicardial layer in Fig. 5). The latest activation was located at the infarcted anterior wall, which constituted the final common pathway of the reentrant circuit. Finally, the wave front reentered the site of origin across the anterior septum to form circuit excitation (arrows in Figs. 5 and 6). The orientation of the reentrant final pathway was from the LV to RV. Epicardially delivered Nd:YAG laser photocoagulated the myocardium in the infarcted anterior wall of the LV along the septum. A linear lesion (12 × 47 mm) was created parallel to the long axis of the heart, perpendicular to the final pathway (black and white lines in Fig. 6). Laser ablation finally eliminated the VT. Multiple intramural electrograms in Figure 7 selected from the same sites as in Figure 5 illustrate that pandiastolic activity disappeared during an induced premature beat after ablation.

Photoablation of Focal Activation Patterns of VT

In eight of 10 canines, nine induced VTs with distinct morphologies were focal activation pat-

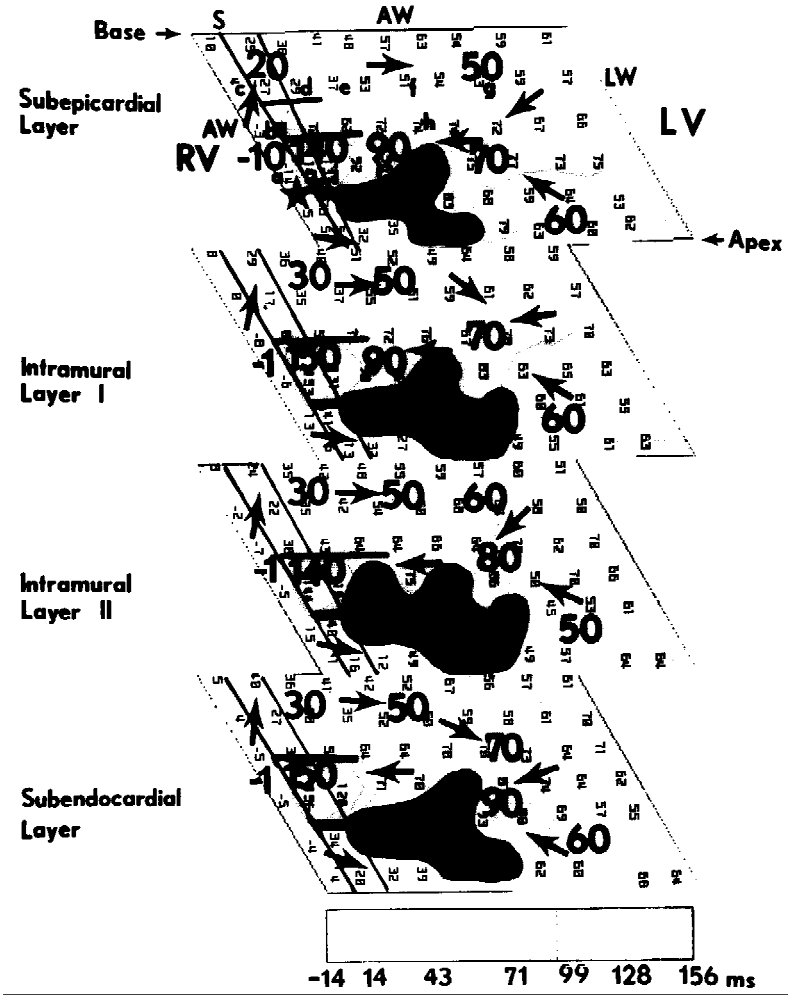

Fig. 5. A 3-D ventricular activation map of a beat (outlined in ECG I in Fig. 4) during induced macro-reentrant VT before photoablation. Four planes in this map indicate the four layers of the regional anterior wall of both ventricles from the subendocardium to the subepicardium.

terns (Table 1). Six focal VTs were eliminated by epicardially delivered laser photocoagulation. Here is an example. Sustained monomorphic VT with a cycle length of 190 ms was induced by electrical stimulation (S1–S2: 300–180 ms). A 3-D activation map (Fig. 8) shows that the activation originated from the apical anterior wall of the RV along the septum (asterisk in level IV). Wave fronts spread radially from the RV to LV, and terminated at the basal lateral wall of the LV (indicated by arrows). Epicardially delivered Nd:YAG laser irradiated the myocardium in the anterior wall of the RV along the septum to form a linear lesion (12 × 67 mm), parallel to the long axis of the heart. Sustained VT was repeatedly terminated during photoablation. The focal VT could no longer be induced after sequential initiation and ablation.

Pathology

To ablate 16 distinct morphologic VTs in 10 canines, 17 photocoagulation lesions were created by epicardially delivered Nd:YAG laser. All of these lesions were in linear shape on the epicardial surface with 8–14 mm wide and 50–72 mm long. In ablation of macro-reentrant VT, nine lesions were created in the infarcted anterior wall of the LV, in which five lesions were parallel to the long axis of the heart, and four were perpendicular to it. In ablation of focal VT, six of eight lesions were located in the anterior wall of the RV along the septum, parallel to the long axis of the

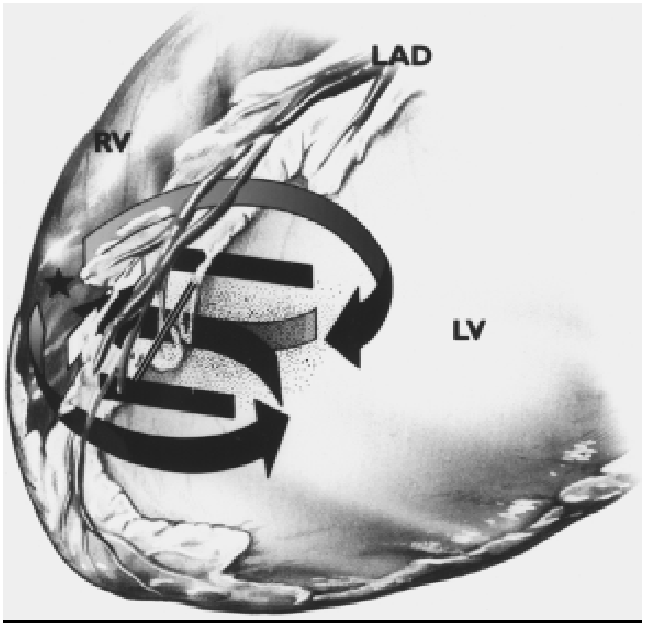

Fig. 6. Schematic illustration of the heart indicating the transeptal reentrant activation sequences of VT in Figure 5 before photoablation. Asterisk indicates the site of origin. Thick black lines represent the regional functional conduction block. The lines in black and white represent the position of photocoagulation lesion.

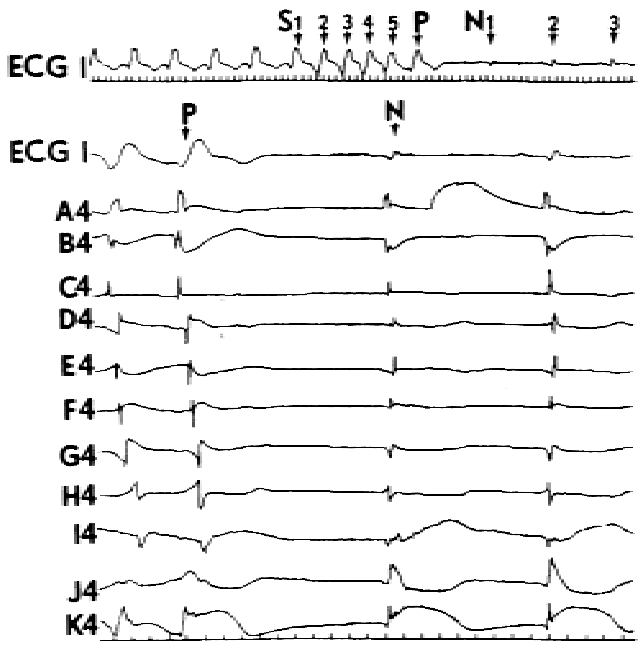

Fig. 7. Surface ECG lead I and multiple intramural electrograms during electrical stimulation after sequential photoablation of VT in Figures 4–6. A premature ventricular complex (indicated by "P") was induced. Delayed activity spanning the entire diastolic interval during premature beat cannot be found in the same leads as in Figure 4. N, normal sinus beats.

heart; two lesions were in the infarcted anterior wall of the LV, perpendicular to the long axis. All photocoagulation lesions were examined by a pathologist. The characteristic pathologic findings were: 1) coagulation lesions in the RV were transmural (Fig. 9); 2) in the outer 10–50% of the infarcted anterior wall thickness, viable muscle could be found with crypts or islands extending into the infarction area (Fig. 10). Occasionally, surviving subendocardium was identified. Laser photocoagulation involved all surviving subepicardial and intramural fibers (Fig. 10). The surviving myocardium might be the arrhythmogenic substrate responsible for post-infarction VT.

DISCUSSION

Identification of the Variable Activation Patterns of Post-Infarction Ventricular Tachycardia

In ablation of post-infarction VT, there are two critical points in influencing the results: identification and ablation. With the help of a computerized mapping system, 240 intramural electrical signals derived from regional or global ventricular walls are simultaneously acquired and analyzed. A variety of activation patterns of induced, post-infarction VT have been recognized [12–17].

Reentrant excitation has long been considered as the major mechanism of VT associated with myocardial infarction. In 2-D epicardial mapping studies [14], figure eight reentrant configuration is described as two circulating wave fronts around arcs of functional conduction block that coalesce into a final common reentrant pathway. In the present study, seven of 16 induced post-infarction VTs with distinct morphologies are due to macro-reentrant excitation. Identification of the orientation of the final pathway seems to play an important role in ablation of VT. In these seven macro-reentrant VTs, final pathways were all located in the infarcted anterior wall of the LV, in which four were perpendicular to the long axis of the heart, and three parallel to it.

The activation sequences of focal VT display that an impulse originates from the focal myocardium, spreads radially to the entire ventricles with or without slow conduction [13,16–17]. Focal patterns of VT have been found to be present in acute, subacute, and chronic myocardial infarc-

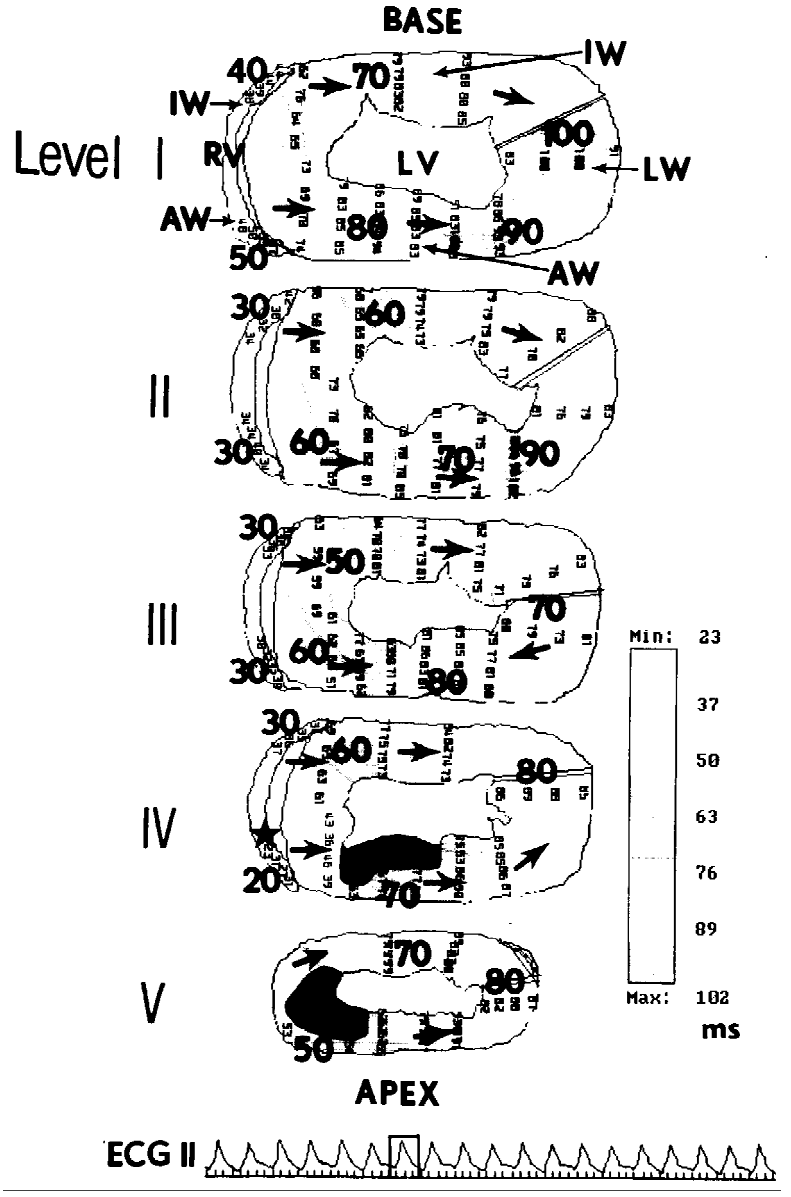

Fig. 8. A 3-D ventricular activation map of a beat during sustained VT induced by electrical stimulation. The map demonstrates that the wave fronts of VT originate from the apical anterior wall of the right ventricle (asterisk in level IV), and spread radially to the entire heart.

tion in both animals and humans [13,16–17]. Multiple focal activation patterns have been revealed in computerized 3-D cardiac mapping studies [13]. In the present study, nine of 16 induced, sustained monomorphic VTs are attributed to focal excitation. The sites of origin are identified in the apical anterior wall of the RV along the septum in eight VTs, and in the anterior wall of the LV in one VT.

Ablation of the Variable Activation Patterns of Post-Infarction Ventricular Tachycardia

Many interventional procedures have been established to ablate post-infarction VT [3–11]. Catheter ablation is an attractive procedure since many of inexpensive energy sources can be used in less equipped hospitals. However, catheter ablation of VT has a low success rate (20.6%) [3].

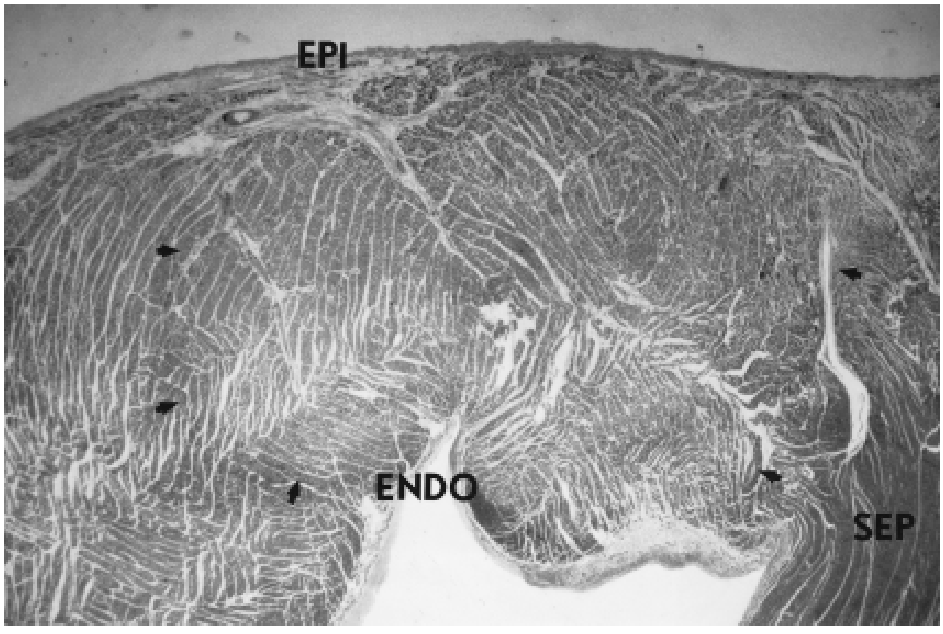

Fig. 9. Histological section of a segment of transmural photocoagulation lesion in the right anterior wall adjacent to the septum indicated by arrows (original magnification, ×12.5, Masson's trichrome stain). EPI, epicardium; ENDO, endocardium; SEP, septum.

Radiofrequency catheter ablation lesion is usually less than 1 cm^2 in surface size, non-transmural and discreet [22–23]. DC ablation, which involves other risks, can create transmural lesions with a 2.0–3.4 cm^2 surface size [24]. These lesions may be too small to ablate the arrhythmogenic tissues. In surgical ablation of VT in patients, ventricular myocardial tissues with about 20–60 cm^2 in surface size are resected guided by 2- or 3-D intraoperative mapping [17,25]. Removing such large areas of myocardial tissues often makes a cardiologist suspicious as to whether it is necessary to do the intraoperative mapping during surgical ablation of VT at all [26]. In the present study, we assumed that transection of the final pathway in reentrant VT or destruction of the site of origin in focal VT would finally ablate post-infarction VT. Histopathologic examination demonstrates that photocoagulation lesions are located at the infarcted anterior wall of the LV, or at the anterior wall of the RV along the septum. Lesions are in linear shape with an average size of 691–750 mm^2 on the epicardial surface (Table 1). These lesions are larger than radiofrequency lesions, and much smaller than lesions made by surgical resection.

Several factors influence the final ablation results: 1) the orientation of the final pathway in reentrant VT or the site of origin in focal VT are correctly identified; 2) transmural lesions have been created in the target areas; 3) the numbers of distinct morphologic VT can be induced in a heart. The more induced VTs, the more likely the infarcted heart is to fail; 4) both infarct size and cardiac function are other important factors.

Limitations and Implications

From a strictly scientific point of view, there are some limitations to this study. First, the long-term success and side effects of the ablation remain unknown. Second, on-line analysis of 240 intramural electrograms and generation of a 3-D activation map is time-consuming work. Insertion of plunge needles into the heart is very invasive. These limitations in methodology will limit the clinical application.

Based on on-line analysis of 3-D activation sequences of induced post-infarction VT in canines, epicardially delivered Nd:YAG laser irradiates the areas of the final pathway in reentrant VT and the site of origin in focal VT; 13 of 16 post-infarction VTs are successfully ablated. The current experiments supply the direct evidence that epicardially delivered laser energy, in conjunction with electrical activation mapping, has a high probability of ablating post-infarction ventricular tachycardia. This study may have an important implication in guiding catheter ablation

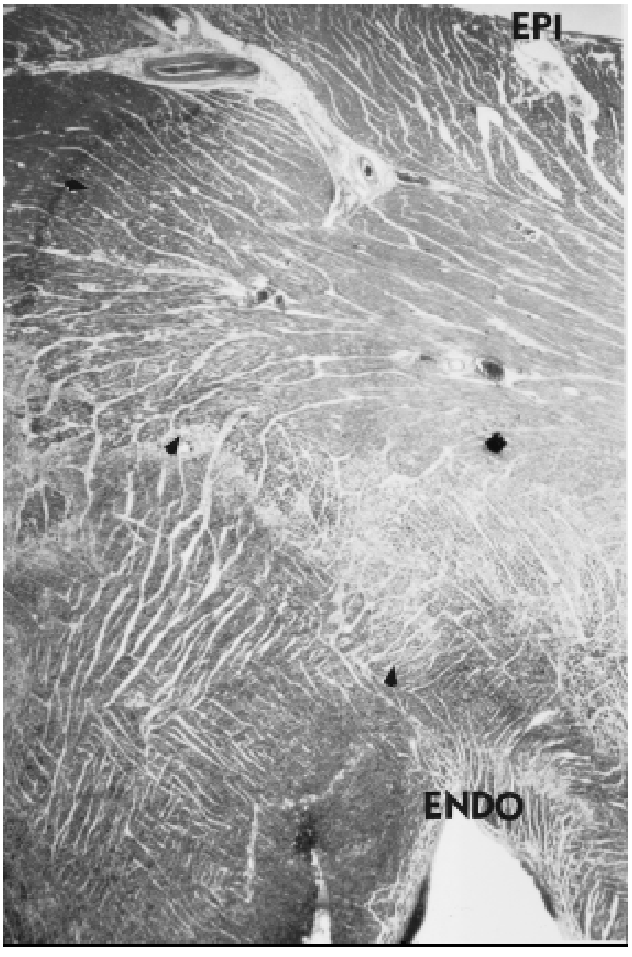

Fig. 10. Histological section of a segment of photocoagulation lesion in the left anterior wall. Half of the epicardial-side ventricular wall having surviving myocardium, was rendered necrotic by Nd:YAG laser irradiation (original magnification, ×12.5, Masson's trichrome stain).

of malignant post-infarction ventricular tachycardia in patients.

REFERENCES

1. Julian DG, Valentine PA, Miller GG. Disturbances of rate, rhythm and conduction in acute myocardial infarction: A prospective study of 100 consecutive unselected patients with the aid of electrocardiographic monitoring. Am J Med 1964; 37:915–927.
2. Luna AB, Coumel P, Leclercq JF. Ambulatory sudden cardiac death: mechanisms of production of fatal arrhythmia on the basis of data from 157 cases. Am Heart J 1989; 117:151–159.
3. Blanchard SM, Walcott GP, Wharton JM, Ideker RE. Why is catheter ablation less successful than surgery for treating ventricular tachycardia that results from coronary artery disease? PACE 1994; 17[Pt. I]:2315–2335.
4. Callans DJ, Schwartzman D, Gottlieb CD, Marchlinski FE. Insights into the electrophysiology of ventricular tachycardia gained by the catheter ablation experience: "Learning while burning". J Cardiovasc Electrophysiol 1994; 5:877–894.
5. Svenson RH, Littmann L, Gallagher JJ, Selle JG, Zimmern SH, Fedor JM, Colavita PG. Termination of ventricular tachycardia with epicardial laser photocoagulation: a clinical comparison with patients undergoing successful endocardial photocoagulation alone. J Am Coll Cardiol 1990; 15:163–170.
6. Littmann L, Svenson RH, Gallagher JJ, Selle JG, Zimmern SH, Fedor JM, Colavita PG. Functional role of the epicardium in postinfarction ventricular tachycardia. Observations derived from computerized epicardial activation mapping, entrainment, and epicardial laser photoablation. Circulation 1991; 83:1577–1591.
7. Guiraudon G, Fontaine G, Frank R, Escande G, Etievent P, Cabrol C. Encircling endocardial ventriculotomy: a new surgical treatment for life-threatening ventricular tachycardias resistant to medical treatment following myocardial infarction. Ann Thorac Surg 1978; 26:438–444.
8. Landymore RW, Gardner MA, McIntyre AJ, Barker RA. Surgical intervention for drug-resistant ventricular tachycardia. J Am Coll Cardiol 1990; 16:37–41.
9. DiMarco JP. Management of sudden cardiac death survivors: role of surgical and catheter ablation. Circulation 1992; 85:I125–I130.
10. Ferguson TB. The future of arrhythmia surgery. J Cardiovasc Electrophysiol 1994; 5:621–634.
11. Stevenson WG, Khan H, Sager P, Saxon LA, Middlekauff HR, Natterson PD, Wiener I. Identification of reentry circuit sites during catheter mapping and radiofrequency ablation of ventricular tachycardia late after myocardial infarction. Circulation 1993; 88:1647–1670.
12. Wu G, Littmann L, Svenson RH, Nanney G, Tatsis GP, Tuntelder JR, Chuang CH, Thompson M, Dezern KR. Ventricular tachycardia due to intramural figure eight reentry revealed by computerized three dimensional electrical activation mapping. Proceedings of IEEE Engineering in Medicine and Biology 1994; 16:11–12.
13. Wu G, Littmann L, Svenson RH, Tatsis GP, Nanney GA, Tuntelder JR, Thompson M, Dezern KR. Intramural activation patterns of focal ventricular tachycardia induced by programmed stimulation during experimental subacute myocardial infarction. J Am Coll Cardiol 1995; 24: 249A.
14. El-Sherif N, Restivo M, Gough WB. The figure-of-eight model of reentrant ventricular rhythms in the subacute phase of myocardial infarction. In: Shenasa M, Borggrefe M, Breithardt G, ed. "Cardiac Mapping." Mount Kisco, NY: Futura Publishing Company, Inc., 1993, pp 159–182.
15. Wit AL, Dillon SM. Anisotropic reentry. In Shenasa M, Borggrefe M, Breithardt G, ed. "Cardiac Mapping." Mount Kisco, NY: Futura Publishing Company, Inc., 1993, pp 127–154.
16. Pogwizd SM. Focal mechanisms underlying ventricular tachycardia during prolonged ischemic cardiomyopathy. Circulation 1994; 90:1441–1458.
17. Pogwizd SM, Hoyt RH, Saffitz JE, Corr PB, Cox JL, Cain ME. Reentrant and focal mechanisms underlying ventricular tachycardia in the human heart. Circulation 1992; 86:1872–1887.
18. Svenson RH, Gallagher JJ, Zimmern SH, Fedor J, Har-

bold N, Elliott C, Hall D, Austin K, Thomley A, Wilson BH, Selle J. Intraoperative Nd:YAG laser photocoagulation ablation of ventricular tachycardia: observations relevant to transcatheter ablation techniques. J Am Coll Cardiol 1987; 9:249A.

19. Svenson RH, Littmann L, Colavita PG, Zimmern SH, Gallagher JJ, Fedor JM, Selle J. Laser photoablation of ventricular tachycardia: correlation of diastolic activation times and photoablation effects on cycle length and termination—Observations supporting a macroreentrant mechanism. J Am Coll Cardiol 1992; 19:607–613.
20. Littmann L, Svenson RH, Chuang CH, Splinter R, Kempler P, Norton J, Tuntelder JR, Thompson M, Tatsis GP. Neodymium:YAG contact laser photocoagulation of the in vivo canine epicardium: dosimetry, effects of various lasing modes, and histology. Lasers Surg Med 1993; 13: 158–167.
21. Wu G, Littmann L, Svenson RH, Nanney GA, Tatsis GP, Tuntelder JR, Chuang CH, Thompson M, Dezern KR. Computerized three dimensional activation mapping study of spontaneous ventricular arrhythmias during acute myocardial ischemia in dogs—Evidence against macro-reentrant mechanism. J Electrocardiol 1995; 28: 115–130.
22. Haines DE. Determinants of lesion size during radiofrequency catheter ablation: the role of electrode tissue contact pressure and duration of energy delivery. J Cardiovasc Electrophysiol 1991; 2:509–515.
23. Oeff M, Langberg JJ, Franklin JO, Chin MC, Sharkey H, Finkbeiner W, Herre JM, Scheinman MM. Effects of multipolar electrode radiofrequency energy delivery on ventricular endocardium. Am Heart J 1990; 119:599–607.
24. Scheinman MM, Laks MM, DiMarco J, Plumb V. Current role of catheter ablative procedures in patients with cardiac arrhythmias: a report for health professionals from the subcommittee on electrocardiography and electrophysiology, American Heart Association. Circulation 1991; 83:2146–2153.
25. Krafchek J, Lawrie GM, Roberts R, Magro SA, Wyndham CRC. Surgical ablation of ventricular tachycardia: improved results with a map-directed regional approach. Circulation 1986; 73:1239–1247.
26. Thakur RK, Guiraudon GM, Klein GJ, Yee R, Guiraudon CM. Intraoperative mapping is not necessary for VT surgery. PACE 1994; 17:2156–2162.